A Nature Inspired Optimization for Retinal Lesion Detection

Kanchan S. Gorde [1,2,*] and Ajay A. Gurjar [1]

[1] Department of Electronics and Telecommunication Engineering,
Sant Gadge Baba Amravati University, Maharashtra, India
[2] Department of Electronics Engineering, Terna Engineering College, University of Mumbai, India
Email: kanchangorde@ternaengg.ac.in (K.S.G.); prof_gurjar1928@rediffmail.com (A.A.G.)
*Corresponding author

***Abstract*—Diabetic retinopathy ranks among the most prevalent preventable causes of blindness worldwide. Failure to detect this condition early on can lead to permanent vision loss. With the increasing number of diabetic patients, there's a pressing challenge due to the scarcity of ophthalmologists. To assist these professionals in decision-making, the development of an automated Diabetic Retinopathy (DR) screening system is recommended. A key aspect of diagnosing diabetic eye disease involves identifying retinal lesions, particularly hard exudates. Proposed research suggests employing an advanced Genetic Algorithm, leveraging Egyptian Vulture Optimization (EVO), and a ResNet-based U-Net model to detect hard exudates in retinal images for early-stage retinopathy diagnosis. The study utilizes the IDRiD retinal image database for training and validation, with the e-Ophtha dataset serving as the test images for the proposed algorithms. Results from the IDRiD set demonstrate an Intersection over Union (IoU) score of 89.5 and a loss of 0.149, while the e-Ophtha dataset yields an IoU score of 77.2 and a loss of 0.29. This innovative approach, trained with a limited number of images, outperforms existing learning algorithms, showcasing promising potential for enhanced diabetic retinopathy diagnosis.**

***Keywords*—fundus image, diabetic retinopathy, machine learning, optimization algorithm**

I. INTRODUCTION

Diabetic Retinopathy (DR) stands as a significant contributor to blindness, stemming from heightened blood glucose levels. As per the American Academy of Ophthalmology, the population afflicted with diabetes mellitus is estimated to reach 387 million and possibly surge to 592 million by 2035. The occurrence of DR is reported at 77.3% for type 1 and 25.1% for type 2 diabetes [1]. Early signs of DR are absent, making early detection imperative for preserving vision. Some individuals notice changes such as difficulty reading or focusing on distant objects [2]. In advanced stages, retinal blood vessels may bleed into the vitreous, filling the eye with a gel-like substance [3]. Global prevalence studies [4] indicate a DR prevalence of 22.27% and vision-threatening DR at 6.17%. It was anticipated that by 2020, the worldwide count of adults affected by DR and vision-threatening DR would reach 103.12 million and 28.54 million, respectively. Projections suggest these figures could rise to 160.50 million and 44.82 million by 2045. Despite medical advancements, diabetic retinopathy remains a prevalent complication of diabetes mellitus and a leading cause of preventable blindness among the working-age adult population [1, 4].

Hard Exudates (HE) found in the retina signify the presence of DR. These bright lesions form as wax-like and proteinaceous substances breach the compromised blood retinal barrier.

The majority of Hard Exudates (HE) typically localize in the outer layers of the retina's plexiform structure [5]. Optical Coherence Tomography (OCT) serves as a tool for detecting HE as hyper-reflective foci, sometimes visible during fundus examination even in the absence of corresponding hard exudates [6]. These hyper-reflective foci, when compared to histology, may serve as early signs of lipoprotein extravasation due to breakdown of the inner blood-retinal barrier [7].

Individuals exhibiting subretinal hyper-reflective foci in Spectral Domain optical Coherence Tomography (SD-OCT) and Diabetic Macular Edema (DME) may eventually develop subfoveal deposition of hard exudates. SD-OCT offers an imaging modality for early detection of DR indicators and macular edema, aiding in understanding the progression of retinal edema and hard exudates [8]. The Early Treatment for DR Study (ETDRS) highlights a correlation between elevated serum lipid levels and increased risk of HE within eyes affected by DR, with vision impairment risk escalating as exudate levels rise.

The International Council of Ophthalmology's 2020 report reveals a concerning shortage of ophthalmologists in India, with 23,000 practitioners for 60 million DR patients, underscoring the need for automated DR detection techniques to catch the disease in its early stages. While Computer-Aided Systems for DR detection employ image processing algorithms, their reliance on handcrafted features and susceptibility to variations in image quality and pathology limit their robustness.

Manuscript received December 30, 2023; revised March 23, 2024; accepted April 22, 2024; published October 21, 2024.

Recent advances in Machine Learning (ML) have facilitated precise DR detection and categorization through automated diagnosis approaches. Early-stage detection of HE in color retinal images holds promise for preventing retinal damage, albeit challenging due to similarities with other fundus structures. Deep learning methods necessitate extensive datasets for accurate DR detection. Analyzing retinal OCT images for highly reflective areas indicative of hard exudates offers an automated approach [9]. The proposed method, focusing on assessing the shadowing effect of hard exudates, presents an alternative to relying solely on brightness spots for detection.

Optimization algorithms provide robust, interpretable, adaptable, and efficient solutions for clinical practice [10]. Dealing with large datasets can be computationally demanding. In Ref. [11], a Convolutional Neural Network (CNN) is employed to forecast the progression of lesions associated with abnormal retinal blood flow. Neural Networks (NN) serve as cost-effective tools for detecting Diabetic Retinopathy (DR), lessening the burden of diabetic eye screenings.

The proposed study aims to develop a precise and resilient system for hard exudate detection by combining Nature-Inspired Optimization Algorithms (NIOA) with ResNet-based networks. NIOA mimics natural phenomena like evolution and group behavior to swiftly find near-optimal solutions compared to deep learning methods. ResNet-based networks adeptly capture intricate image features, while U-Net architecture excels in segmentation tasks by preserving spatial information, facilitating efficient learning even with limited annotated data [6]. By amalgamating optimization algorithms' strengths with neural networks, diabetic retinopathy detection is enhanced through automated parameter optimization, improved interpretability, and the creation of robust models. The proposed approach's superior performance is confirmed through comparisons with existing algorithms in hard exudate detection (see Fig. 1).

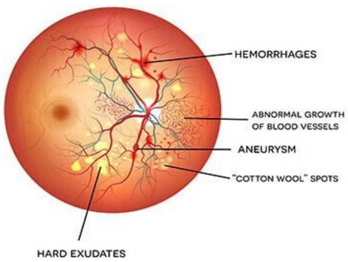

Fig. 1. Diabetic retinopathy fundus [5].

II. Literature Review

A two-stage framework is proposed [12] for diagnosing diabetic macular edema in retinal images. Firstly, exudates are segmented, and a centered region with the highest probability is cropped. The impact of image cropping, ranging from 240×240 to 1200×200 pixels, is then examined by cropping maximum probability pixel-varying regions and setting thresholds to determine the corresponding assessment results.

Another system for exudate identification employs pre-trained convolutional neural networks [13]. Localizing exudate features is aided by Region-of-Interest (ROI) localization, followed by feature extraction using transfer learning with CNN models that have already undergone training. The SoftMax classifier is then applied to categorize exudates based on combined properties from the Fully Connected (FC) layers.

To identify all stages of diabetic retinopathy using both symmetrical and asymmetrical datasets, two Deep Convolutional Neural Network (DCNN) models were proposed [14]. These models were developed using the Kaggle dataset for training, integrating data from advanced Graphical Processing Systems. Various batch sizes were employed during model training, with performance measures showing variations corresponding to batch size.

Using a larger batch size can enhance the accuracy of models. Recently, various automated techniques have been employed, including Xception [15], K-Nearest Neighbors (KNN) and Support Vector Machine (SVM) [16], modified FCN-8 [17], and residual network [18], to identify and categorize lesions associated with diabetic retinopathy.

A novel method for detecting hard exudates is presented, utilizing the nature-inspired algorithm, Egyptian Vulture Optimization (EVO) [19]. This approach yields faster results for hyperparameter convergence compared to existing methods. By leveraging the diversity-promoting mechanisms of EVO, the genetic algorithm (GA) explores the solution space more comprehensively. The proposed Hard Exudate (HE) detection system employs the ResNet-based Siamese U-Net model for segmentation tasks, as the dataset used is relatively small and binary in nature. Originally developed for segmenting biological images, the U-Net algorithm [20] is adept at this task. The Siamese network compares pairs of retinal images to detect subtle changes. Through the integration of these model architectures, the proposed method extracts discriminative features, achieving precise segmentation that facilitates accurate detection of hard exudates. This enables clinicians to visualize and analyze these lesions for the early diagnosis of diabetic retinopathy.

III. Proposed Methodology

The methodology described relies on nature-inspired algorithms and pretrained residual network models for detecting hard exudates in retinal images. U-Net, a well-established network for extracting pixel-level information in segmentation tasks [21], is employed as a Siamese network to ensure similarity in detected features from both images, with a fully connected layer on top facilitating this process. Hyperparameter optimization is conducted using a genetic algorithm enhanced by the Egyptian Vulture-based Optimization (EVO) method. The model architecture is constructed using Python's Keras framework, a versatile API for neural networks that offers consistency in building various deep learning models. The best features extracted from the Egyptian Vulture-based Optimization (EEVG) are then applied to the model's training process.

A. Dataset

The proposed study utilizes retinal images sourced from the available Indian Diabetic Retinopathy Image Dataset (IDRiD) fundus image set [22], comprising a training set of 54 exudate images and a testing set of 27 exudate images. For model evaluation, the e-Ophtha dataset [23] is employed, consisting of 35 fundus pictures without lesions and 47 images with exudates.

In the IDRiD dataset, typical fundus structures and Diabetic Retinopathy (DR) lesions are meticulously labeled at the pixel level. This dataset serves as a suitable resource for advancing and evaluating image examination algorithms aimed at early detection of retinopathy. On the other hand, e-Ophtha provides a collection of color retinal images intended for systematic investigation in diabetic retinopathy.

B. Data Pre-processing

Before proceeding to model, essential input image pre-processing is conducted, involving mean shifting and new map image methods.

The *mean shifting* algorithm is initially applied to input fundus images to achieve color normalization. This process enhances visual quality by improving image contrast and adjusting brightness levels towards the mean of the image. A reference image, accurately color-balanced and recorded, serves as the basis for this normalization. The image's channels for Red (R), Green (G), and Blue (B) are separated, and the average values for each channel are determined. These values are then used to adjust the R, G, and B channels in the final dataset images, ensuring consistency across the dataset [24].

$$r_i = \left\{\frac{r_i}{mean(R)} \times R_{mean}, 255\right\} \tag{1}$$

$$g_i = \left\{\frac{g_i}{mean(G)} \times G_{mean}, 255\right\} \tag{2}$$

$$b_i = \left\{\frac{b_i}{mean(B)} \times B_{mean}, 255\right\} \tag{3}$$

To represent the mean value of the R channel in the reference image, R, G, and B are represented for each pixel *i* in each image.

Gamma correction is performed using a reference image to ensure proper adjustments of the image's lightness and darkness. This technique aids in enhancing the overall contrast and highlighting exudates in the images (Fig. 2). Its purpose is to address discrepancies in human eye perception and the linear response of display devices.

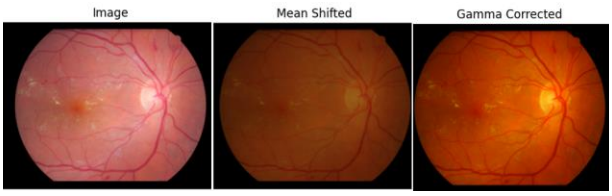

(a) (b) (c)

Fig. 2. Pre-processed Images, (a) IDRiD fundus image [22] (b) Mean Shifted image (c) Gamma corrected.

Map Image is created from a shifted image by performing the following operations:

- Transformed fundus image to LAB color space
- Applied tophat operation on LAB color space image
- Then the operation is performed on the converted image using the following equation:

X = "a" axis from LAB - NOT "R" axis from RGB (4)

Map = NOT (X + tophat) (5)

The LAB color space is utilized to segregate color information from brightness information, offering perceptual uniformity. The Tophat filter is applied to enhance brighter objects within an image. Additionally, a map image is generated to extract optic disc information while preserving bright exudates unaffected.

Following basic pre-processing, images (Fig. 3) are resized to ensure that their maximum width is 640 pixels.

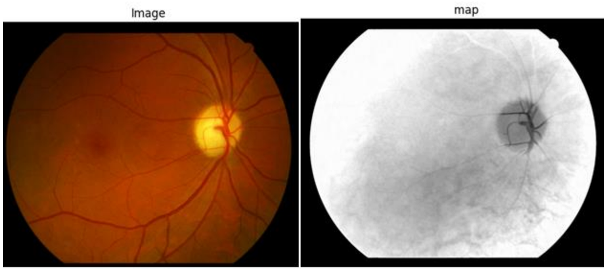

Fig. 3. Original image [22] and processed map image.

C. Optimization Using EEVG

Similar to other avian species, Egyptian vultures primarily feed on meat but also exhibit a unique ability to consume the eggs of other species. They employ ingenious tactics such as tossing pebbles at sturdy eggs, rolling them with twigs, and breaking them at weak points to access the flesh [19]. Inspired by the foraging behavior of Egyptian vultures, the Egyptian Vulture Optimization (EVO) algorithm is designed for locating and consuming food. The framework of the EVO algorithm is illustrated in Fig. 4. Just as the vulture throws stones at tougher eggs until they crack, the algorithm introduces fresh solutions into the solution set at specific intervals, breaking the existing solutions. Subsequently, rolling the solution set induces variations in variable positions, potentially yielding new solutions with enhanced fitness values. This change in angle represents a mutation phase, accomplished by selectively altering the solution subset.

Genetic Algorithms (GAs) draw inspiration from the biological evolution process, involving chromosome representation, fitness selection, and biological-inspired operators such as selection, mutation, and crossover [10]. The EVO algorithm enhances solution diversity and efficiently explores the solution space. Combining EVO with GA prevents premature convergence to local optima by preserving diversity and refining solutions in favorable regions of the search space

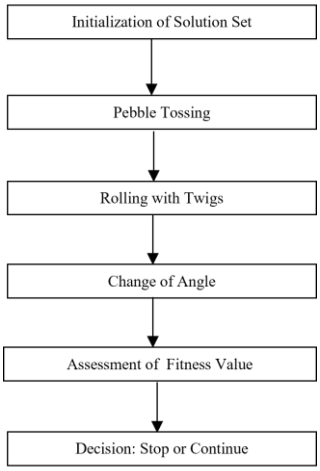

Fig. 4. EVO framework.

The Enhanced Egyptian Vulture-based Genetic (EEVG) algorithm is employed to swiftly identify the optimal hyperparameters for the model through a few iterations of the evolutionary algorithm. In optimization algorithms, hyperparameters are initially set before training begins and remain constant throughout the training process, influencing the model's learning behavior. Hyperparameter tuning is crucial for constructing an effective machine-learning model with an optimal configuration by exploring various possibilities. The aim is to expedite the genetic algorithm process using the steps outlined in the EEVG Optimization algorithm (Fig. 5).

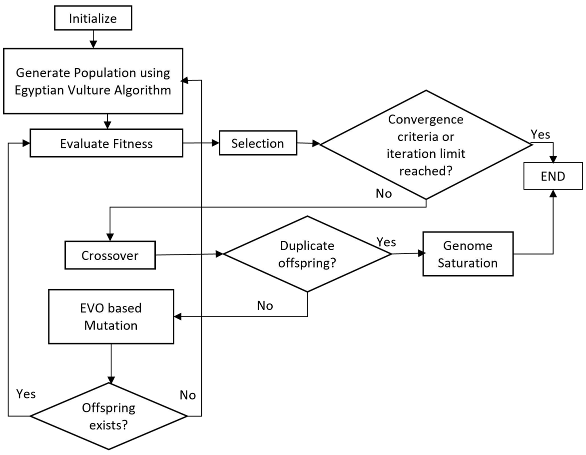

Fig. 5. Proposed EEVG flow.

The proposed EEVG algorithm followed below steps:

- The hyperparameters are encoded into numerical values.
- All encoded hyperparameters are then converted into a byte matrix.
- An initial population is created using EVO mutation, involving actions like tossing pebbles, rolling twigs, and adjusting angles.
- The population undergoes evaluation through model training using the decoded parameters, referred to as the genome.
- Scores are assigned to each set, and top-performing individuals are chosen as parents for crossover to produce offspring.
- The offspring are checked for genome saturation (duplicate offspring). If saturation is reached, additional sets of parents are generated.
- If no duplicate offspring are produced, the EVO-based mutation process continues for further evaluation and selection of the new generation.
- If convergence criteria are met or the maximum number of generations is reached, the Enhanced Egyptian Vulture-based Genetic (EEVG) algorithm terminates.

D. Data Splitting

In the IDRiD dataset, the data is split into two phases: training and validation. The training set consists of 54 images, while the validation set comprises 27 images. For testing the proposed work, the e-Ophtha dataset, which contains 47 images with exudates, is utilized [25].

E. Hyper Parameters

The following hyperparameters are used for selected architectures and their specified values used for research work are shown in Table I:

TABLE I. HYPER PARAMETERS USED FOR EEVG

Hyperparameters	**Value**
Batch Size	4, 8, 16
Learning Rate	0.001, 0.01, 0.005
Batch normalization	true, false
Convolutional Layer Initializers	uniform, normal, glorot_normal, glorot_uniform, he_normal, he_uniform
Final Layer Initializer	uniform, normal, glorot_normal, glorot_uniform, he_normal, he_uniform
Optimizer	adam, sgd

- *Batch Size:* The number of samples used in each iteration of the training process and can be adjusted according to dataset size and memory.
- *Learning Rate:* Controls the step size used in the optimization process.
- *Batch Normalization:* The training process improved by normalizing each layer input.
- *Initializers:* The weight of convolutional filters initialized before training the network.
- *Optimizers:* The model weights are updated during training to minimize the loss function.

F. Data Augmentation

Creating updated duplicates of the images within the dataset is termed data augmentation, employed to artificially enhance the diversity within the training dataset. This technique proves highly beneficial when the training data is limited. Augmentation techniques like horizontal flipping, scaling, rotation, and random cropping are applied to the existing dataset to introduce greater variability.

G. Performance Metrics

The performance metrics evaluate the exudate predictions produced by the system against the actual ground truth label data. These metrics are determined based on the True Positive (TP), False Positive (FP), True Negative (TN), and False Negative (FN) values of the picture pixels.

TP: model predicts positive instances as positive correctly

TN: model predicts negative instances as negative correctly

FP: model predicts negative instances as positive incorrectly

FN: model predicts positive instances as negative incorrectly

1) Intersection over Union (IoU)

The degree of intersection between two boxes is quantified as an Intersection over Union (IoU) value. IoU is utilized to evaluate the overlap between the Ground Truth and Prediction regions in the context of object detection and segmentation.

$$IoU = \frac{TP}{TP+FP+FN} \tag{6}$$

2) Dice score and loss

The dice score serves as a comprehensive indicator for projects. It is calculated by taking 2 times the overlapped area and dividing it by the total pixels in both images. This score is equivalent to the F–Score and gauges the comparative overlap between the prediction and the ground truth. Addressing data imbalance in image segmentation, Dice Loss is derived as one minus the dice coefficient, serving as a key metric in this context.

$$Dice = \frac{2\times TP}{2\times TP+FP+FN} \tag{7}$$

3) Accuracy

Accuracy, abbreviated as Acc, quantifies the proximity of a received value to its true value. It assesses the correctness of a model by determining the ratio of correctly classified pixels to the total number of pixels in the image.

$$Accuracy = \frac{TP+TN}{TP+TN+FP+FN} \tag{8}$$

4) Sensitivity (SE) and Specificity (SP)

The sensitivity ratio describes the proportion of true positives to all other positives, akin to how specificity measures the percentage of true negatives to all negatives, the true negative rate serves a similar purpose.

$$Sensitivity = \frac{TP}{TP+FN} \tag{9}$$

$$Specificity = \frac{TN}{TN+FP} \tag{10}$$

IV. Model Selection

The U-Net model is preferred for improved performance due to its ability to extract pixel-level information for segmentation tasks. Utilizing ResNet-based U-Net as Siamese networks ensures similarity in the extracted features from both images. A fully connected layer is subsequently applied atop to fulfill the task. The model architecture is constructed using the Keras framework. Extracting the best features from EEVG, this information is then utilized to train the final model.

A. Residual Network (ResNet)

ResNet, a deep neural network, addresses the issue of vanishing gradients by incorporating residual blocks, which include shortcut skip connections to bypass certain layers, thereby minimizing information loss [26]. This architecture enables the extraction of intricate feature maps, enhancing feature extraction capabilities through cross-layer feature fusion. As the network grows deeper, its performance progressively improves.

B. Siamese Network

A Siamese network is a symmetric neural network comprising two or more like sub networks with shared weights. Its purpose is to determine the similarity between pairs of input images. Through training, this network learns to distinguish a new class even with limited examples.

C. U-Net Architecture

U-Net, Convolutional Neural Network (CNN) architecture, serves to classify each pixel in an image into a specific object category. Its U-shaped design, featuring both a contracting and expanding path, facilitates context capture and precise localization. Incorporating skip connections between these paths allows for the integration of data from various scales. Despite a limited number of training samples, U-Net demonstrates accurate segmentation.

The presented approach combines these networks into what is termed as ResNet-based Siamese U-Net. This model integrates ResNet for robust feature extraction, Siamese architecture for comparing features extracted from retinal images, and U-Net for precise semantic segmentation of lesions, thereby accurately detecting hard exudates in retinal images. This method enables comprehensive analysis and diagnosis of diabetic retinopathy with high accuracy and efficiency.

The ResNet-based Siamese U-Net architecture is depicted in Fig. 6. Steps followed to complete the proposed work are as below:

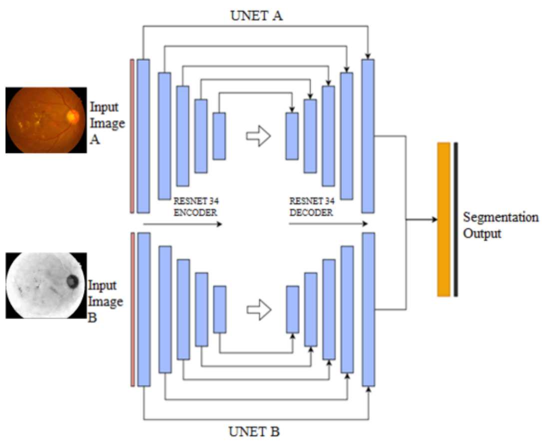

Fig. 6. ResNet-based Siamese U-Net model.

- Load the dataset and perform the required pre-processing;
- Build the model;
- Run EEVG to get the best-fit parameters;
- Use the best parameter sets to train the model;
- Test for unseen datasets and evaluate the score.

V. Result and Analysis

To assess the effectiveness of the proposed approach, two public datasets are utilized: IDRiD, comprising 54 fundus images with exudate lesions, and the e-Ophtha dataset, which contains 47 exudate images. In Fig. 7, the plot illustrates the dice loss about iterations, with blue dots representing the dice loss and a red dotted line indicating the trend of generation. It is observed that the loss value consistently decreases with each iteration of generation. The utilization of Egyptian Vultures optimization introduces higher yet correlated mutations, resulting in faster and more efficient exploration of potential parameter sets across all possibilities. As a result, decent results are achieved within just 10 generations.

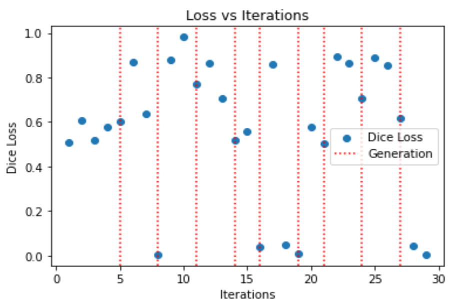

Fig. 7. Loss vs Iteration graph.

Table II displays the performance metrics results for IDRiD Train Set & Test Set, and e-Ophtha exudates fundus image dataset.

TABLE II. Performance Metrics Evaluation

Dataset	IoU	Dice loss
IDRiD - Train set	89.5%	0.1494
IDRiD - Test set	83.9%	0.2146
e-Ophtha	77.2%	0.2904

Fig. 8 showcases selected samples from the e-Ophtha retinal image sets, demonstrating the inference results obtained after testing the proposed method. The first row displays the original e-Ophtha images, the second row presents the ground truth masks sourced from the dataset [23], and the third row depicts the predicted results from the EEVG-ResNet approach. Blue markings on the result images highlight hard exudates on the retina. It is evident that the predicted exudate lesions closely match those delineated in the provided image masks.

Diabetic retinopathy hard exudates detection methods are compared with the proposed EEVG-ResNet-based Siamese U-Net in Table III.

Existing nature-inspired algorithms: Ant Colony Optimization (ACO)-CNN [32], CNN-Enhanced MothFlame Optimization (EMFO) [33], and Particle Swarm Optimization (PCO)-CNN [34] are compared with our EEVG-Res-U-Net algorithm for detection of diabetic retinopathy in Table IV.

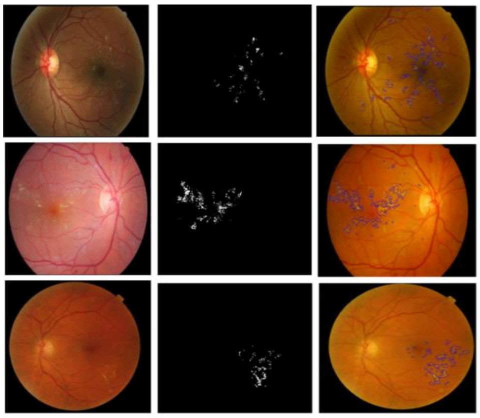

Fig. 8. Result of EEVG-ResNet-based Siamese U-Net on e-Ophtha images, (a) Original image, (b) Ground truth image, (c) HE Detected image.

TABLE III. Performance Comparison of HE Detection Methods

Reference	Method	Metrics
[12]	Cascaded Deep NN	F–Score = 90.5 SE = 92.3
[15]	Xception	Acc. = 83
[16]	KNN, SVM	Acc. = 90
[17]	MFCN-8	SE = 81.7
[18]	ResNet-18	Acc. = 70
[27]	OMRBS	F–Score = 60.9 AUC = 93.4
[28]	CNN	AUC = 92
[29]	CN fusion	F–Score = 78
[30]	U-Net	IoU = 69.8
[31]	ML-FEC	F–Score = 72.8
Proposed work	EEVG-ResNet Siamese U-Net	Testing set: AUC = 95.2 IoU = 77.2 F–Score = 70.9 Acc = 99.7
		Validation set: AUC = 94.9 IoU = 83.9 F–Score = 80.6 Acc = 99.1

TABLE IV. Results for DR Detection Using Nature-Inspired Algorithms

Method	Accuracy (%)	Sensitivity (%)	Specificity (%)
ACO-CNN [32]	91.32	72.53	72.53
DCNN-EMFO [33]	82.00	89.11	58.65
PSO-CNN [34]	97.75	94.80	98.63
EEVG-ResNet based Siamese U-Net	99.76	66.78	99.86

VI. Computation Time

The EEVG algorithm takes approximately 4 h and 20 min to determine the best-fit hyperparameters on the Tesla T4 GPU. Training the proposed network for 50 epochs requires about 2 h and 10 min Additionally, experiments were conducted on a Google Colab GPU, where performance evaluation and optimal hyperparameter selection took 3 h, while the defined model required 48min for 50 epochs to complete the experimental task. Table V presents a comparison of the training computation times of the proposed algorithm with other published learning methods. The proposed EEVG-ResNet-based Siamese U-Net demonstrates superior performance compared to previously published methods.

TABLE V. COMPUTATION TIME FOR TRAINING

Method	Computation Time	Resource
CN Fusion [29]	10 h	Hardware GPU used
Cascaded NN [12]	8 h	
Proposed work	6.5 h	
CNN [13]	6 h	Google Colab GPU used
Proposed work	4 h	

The simulation result for the IDRiD_61 test image is shown in Fig. 9 to verify the predicted mask with the ground truth image.

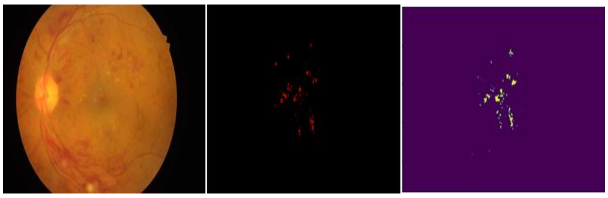

Fig. 9. IDRiD_61 Original image [22], its Ground truth image [22] and predicted mask.

VII. RECEIVING OPERATING CHARACTERISTICS CURVE

A Receiver Operating Characteristic (ROC) curve illustrates the performance of a test in distinguishing true positive rates from false positive rates across different threshold settings of a parameter. The area under the ROC Curve (AUC) serves as a measure of accuracy, indicating the algorithm's capability to discriminate between two classes or groups. Using the presented algorithm and architecture, ROC curves and AUC values for the IDRiD testing set and the e-Ophtha exudates dataset are obtained and depicted in Fig. 10.

Fig. 11 illustrates the Dice loss and IoU score for both training and validation datasets across 50 epochs. Additionally, Fig. 12 showcases the performance metric values including Sensitivity (SE), Specificity (SP), false positive rate, and precision for the training, validation, and testing fundus image datasets.

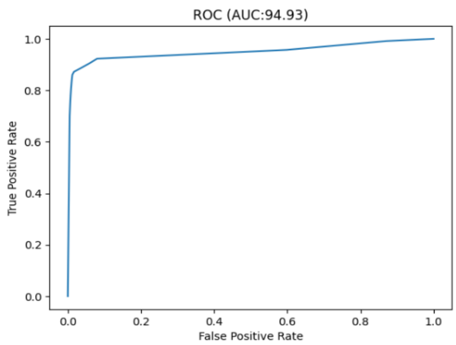

(a)

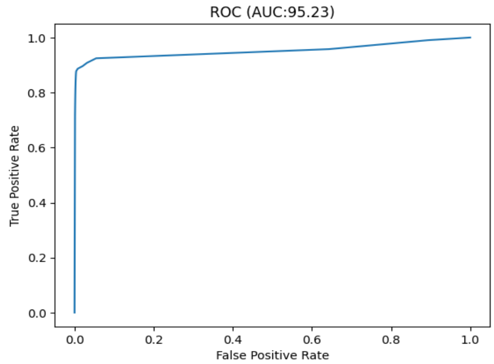

(b)

Fig. 10. ROC Curve, (a) IDRiD testing dataset and (b) e-Ophtha exudates dataset.

(a)

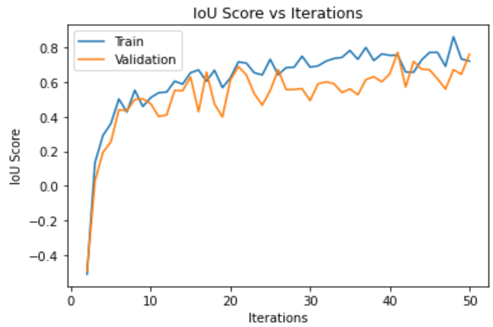

(b)

Fig. 11. Training & validation outputs for metrics: (a) Dice Loss and (b) IoU Score.

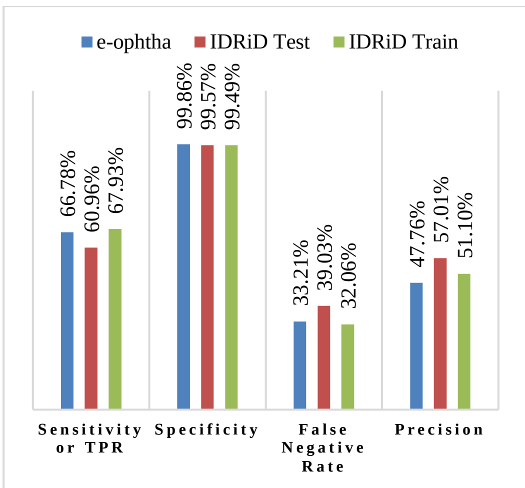

Fig. 12. Performance metrics results for training, validation, and testing datasets.

VIII. CONCLUSIONS

To aid ophthalmologists in decision-making, a nature-inspired automated diabetic retinopathy (DR) detection system has been developed to accurately diagnose DR in its early stages. This research introduces a novel image mapping method that reduces the impact of optic disc brightness during pre-processing to prevent confusion with exudates. Additionally, this work presents a pioneering approach for detecting hard exudates in the retina using the EEVG-based algorithm and Siamese U-Net model. The IDRiD testing set demonstrated an IoU score of 83.9%, a dice loss of 0.2146, and an ROC (AUC) of 94.23, while for the testing dataset e-Ophtha, the proposed algorithm achieved an IoU of 77.2%, a dice loss of 0.294, and an ROC (AUC) of 95.23, values deemed suitable for medical applications. Despite a small training dataset, the presented algorithm outperforms existing methods, achieving validation and testing accuracies of 99.1% and 99.7%, respectively. This method holds promise for detecting other macular diseases in the future.

CONFLICT OF INTEREST

The authors declare no conflict of interest.

AUTHOR CONTRIBUTIONS

Kanchan Gorde conducted the Research, Conceptualization, Methodology, Validation, Formal analysis, Investigation, Data Curation, Writing—Original Draft, Writing—Review & Editing, and Visualization. Ajay A. Gurjar conducted Conceptualization, Investigation, Analysis, and Supervision. All authors had approved the final version.

REFERENCES

[1] S. Anvi and R. Ajay, "Ophthalmology workforce projections in the United States, 2020 to 2035," *American Academy of Ophthalmology*, vol. 131, 2023.

[2] W. Berka, L. Jennifer., and A. G. Miller, "Update on the treatment of diabetic retinopathy," *The Scientific World Journal*, vol. 8, pp. 98–120, 2008

[3] S. I. Pao, H. Z. Lin, K. H. Chien, M. C. Tai, J. T. Chen, and G. M. Lin, "Detection of diabetic retinopathy using channel convolutional neural network," *J. Ophthalmology*, vol. 202, 2020.

[4] Z. L. Teo *et al*., "Global prevalence of diabetic retinopathy and projection of burden through 2045: Systematic review and meta-analysis," *Ophthalmology*, vol. 128, no. 11, pp. 1580–1591, 2021.

[5] A. Benzamin and C. Chakraborty, "Detection of hard exudates in retinal fundus images using deep learning," in *Proc. 2018 Jt. 7th Int. Conf. Informatics, Electron. Vis. 2018 2nd Int. Conf. Imaging, Vis. Pattern Recognition*, 2018, pp. 465–469.

[6] S. Joshi and P. T. Karule, "Biomedicine and pharmacotherapy a review on exudates detection methods for diabetic retinopathy," *Biomed. Pharmacother*, vol. 97, pp. 1454–1460, 2018.

[7] R. Raman, M. G. Nittala, L. Gella, S. S. Pal, and S. T. Retinal, "Sensitivity over hard exudates in diabetic retinopathy," *J. Ophthalmic Vis Res.*, vol. 10, no. 2, pp. 160–164, Apr 2015.

[8] S. Davoudi *et al.*, "Optical coherence tomography characteristics of macular edema and hard exudates and their association with lipid Serum levels in type 2 diabetes," *Retina-The Journal of Retinal and Vitreous Diseases*, vol. 36, no. 9, 2016.

[9] M. Singh *et al.*, "Automatic detection of hard exudates shadow region within retinal layers of OCT images," *Mathematical Problems in Engineering*, 14, 2022.

[10] U. Najib *et al.*, "Diabetic retinopathy detection using genetic algorithm-based CNN features and error correction output code SVM framework classification model," *Wireless Communications and Mobile Computing*, pp. 1–13, 2022.

[11] A. Valizadeh, S. Jafarzadeh Ghoushchi, R. Ranjbarzadeh, and Y. Pourasad, "Presentation of a segmentation method for a diabetic retinopathy patient's fundus region detection using a Convolutional neural network," *Comput. Intell. Neurosci.*, vol. 202, 2021

[12] M. Juan, L. Zhang, and Y. Q. Feng, "Exudate-based diabetic macular edema recognition in retinal images using cascaded deep residual networks," *Neurocomputing*, vol. 290, pp. 161–171, 2018.

[13] M. Mateen, J. Wen, N. Nasrullah, S. Sun, and S. Hayat, "Exudate detection for diabetic retinopathy using pre-trained convolutional neural networks," *Complexity*, vol. 202, 2020.

[14] G. Jinfeng, S. Qummar, Z. Junming, Y. Ruxian, and F. G. Khan, "Ensemble framework of deep CNNs for diabetic retinopathy detection," *Computer. Intelligent. Neuroscience*, vol. 202, 2020

[15] S. H. Kassani, P. H. Kassani, R. Khazaeinezhad, M. J. Wesolowski, K. A. Schneider, and R. Deters, "Diabetic retinopathy classification using a modified xception architecture," in *Proc. 2019 IEEE International Symposium on Signal Processing and Information Technology (ISSPIT), Ajman, United Arab Emirates*, 2019, pp. 1–6.

[16] Y. Reddy and R. Ravindran, "Retinal image lesions assisted diabetic retinopathy screening system through machine learning," *International Journal of Intelligent Engineering and Systems*, vol. 15, no. 2, pp. 175–188, 2022

[17] D. Qomariah, H. Tjandrasa, and C. Fatichah, "Exudate segmentation for diabetic retinopathy using modified FCN-8 and dice loss," *International Journal of Intelligent Engineering and Systems*, vol. 15, no. 2, pp. 508–519, 2022

[18] M. S. Sallam, A. L. Asnawi, and R. F. Olanrewaju, "Diabetic retinopathy grading using ResNet convolutional neural network," in *Proc. 2020 IEEE Conference on Big Data and Analytics (ICBDA)*, Kota Kinabalu, Malaysia, 2020, pp. 73–78.

[19] C. Sur, S. Sharma, and A. Shukla, "Egyptian vulture optimization algorithm – A new nature inspired meta-heuristics for knapsack problem," in *Proc. The 9th International Conference on Computing and Information Technology (IC2IT 2013). Advances in Intelligent Systems and Computing*, 2013, vol. 209, pp. 227–237.

[20] K. He, X. Zhang, S. Ren, and J. Sun, "Deep residual learning for image recognition," in *Proc. IEEE Conference Computer Vision Pattern Recognition*, 2016, pp. 770–778.

[21] O. Ronneberger, P. Fischer, and T. Brox, "U-Net: Convolutional networks for biomedical image segmentation," *Medical Image Computing and Computer-Assisted Intervention*, vol. 9351, 2015.

[22] P. Porwal, S. Pachade, R. Kamble, M. Kokare, G. Deshmukh, V. Sahasrabuddhe, and F. Meriaudeau, "Indian diabetic retinopathy image dataset (IDRiD)," *IEEE Dataport.*, vol. 24, 2018.

[23] D. G. Cazuguel, X. Zhang, G. Thibault, J. C. Klein, F. Meyer, B. Marcotegui, G. Quellec, M. Lamard, R. Danno, D. Elie, P. Massin, Z. Viktor, A. Erginay, B. Laÿ, and A. Chabouis, "TeleOphta: Machine learning and image processing methods for teleophthalmology," *IRBM*, vol 34, pp. 196–203, 2013

[24] I V. Vorobyeva, "Mathematical modeling in diabetic retinopathy," in *Proc. E3S Web of Conferences*, vol. 224, 03020, 2020.

[25] S. M. Khan *et al.*, "Review a global review of publicly available datasets for ophthalmological imaging: barriers to access, usability, and generalizability," *Lancet Digit. Heal.*, vol. 3, no. 1, pp. e51–e66, 2020

[26] J. Z. Liang, "Image classification based on ResNet," *Journal of Physics: Conference Series*, vol. 1634, 012110, 2020.

[27] H. Wang *et al.*, "Hard exudate detection based on deep model learned information and multi-feature joint representation for diabetic retinopathy screening," *Computer Methods and Programs in Biomedicine*, vol. 191, 105398, 2020.

[28] R. Alexander, "Diabetic Retinopathy detection through Integration of deep learning classification framework," bioRxiv preprint, 2017. https://doi.org/10.1101/225508

[29] P. Pavle and S. Lončarić, "Detection of exudates in fundus photographs using deep neural networks and anatomical landmark detection fusion," *Computer Methods and Programs in Biomedicine*, vol. 137, pp. 281–292, 2016.

[30] A. Kushwaha and P. Balamurugan, "Classifying diabetic retinopathy images using induced deep region of interest extraction," in *Proc. 2019 12th International Congress on Image and Signal*

Processing, BioMedical Engineering and Informatics (CISP-BMEI), 2019, pp. 1–6.
[31] U. T. Modupe *et al.*, "Diabetic retinopathy detection using principal component analysis multi-label feature extraction and classification," *International Journal of Cognitive Computing in Engineering*, pp.78–88, 2023.
[32] V. Kumar, "An efficient deep intelligent based MACO-CNN algorithm for classification of diabetic retinopathy disease from retinal fundus images," *Design Engineering*, pp. 5182–5205, 2021.
[33] N. Arun and K. Muthuvel, "automated screening of diabetic retinopathy with optimized deep convolutional neural network: Enhanced moth flame model," *Journal of Mechanics in Medicine and Biology*, vol. 21, no. 1, 2021.
[34] J. Jayanthi *et al.*, "An intelligent particle swarm optimization with convolutional neural network for diabetic retinopathy classification model," *Journal of Medical Imaging and Health Informatics,* vol. 11, no. 3, pp. 803–809, 2021.